

Application of 32-bit SAR A/D Conversion for Vibration, Impact and Shock Datalogging

Leo Bermudez Pestañas, G. Ramana Murthy and A. Kumar Singh
Faculty of Engineering and Technology, Multimedia University,
Jalan Ayer Keroh Lama, 75450 Melaka, Malaysia

Abstract: The measure of mechanical impact, vibration and shock are the few of the important aspect to be considered in designing mechanical moving mechanisms. This is evident on manufacturing plants that can be in the field of semiconductor, automobile, robotics and many more. This vibration, impact and shock measurement parameters are being measured by sensors. The sensor construction may be a strain gauge load cell, piezoelectric or piezoresistive transducer or the latest today is the Microelectro mechanical Systems (MEMS) sensor. The output may be in digital or analog with respect to the amount of G-force produced by such impact on the body. The measurement methods can be either slow or in a fast manner depending on the desired application. All the output of these sensors are then required to be digitized in order for the digital computing device for perform data evaluation. In this study, this will introduce a new technology in Successive Approximation Register (SAR) Analog to Digital (A/D or A-D) converter that can make the digitized the output of the vibration, impact or shock sensor with no missing codes on a 32-bit resolution digital representation while taking samples in a fast manner providing a more smoother readout of impact, vibration or shock subject sources.

Key words: Strain gauge load cell, piezoelectric transducer, microelectromechanical systems, successive approximation register analog to digital converter, G-force, desired application

INTRODUCTION

Vibration impact and shock are the few important parameters to be considered in designing a mechanical machines on human's daily activities. These measurement parameters plays a key role in implementing a good ergonomic technique features of any machines designed regardless of their size. The study of impact and shock are useful when predicting the critical point of a mechanism if in the future it will have cracks and how it will progress. Most of this vibration, shock and impact are being measured by different types of accelerometers or strain gauge load cells.

Most of early accelerometers measures only one axis of motion and were severely limited to the amount of time that could be continuously measured. Many of the newer generation of accelerometers today are highly sensitive and can measure acceleration in multiple planes and allow for a longer duration of continuous data collection (Stinson *et al.*, 2012).

Accelerometers as the name suggests, measures acceleration. Typically they contain a small mass, connected to a stiff spring with some electrical means of measuring the spring deflection when the mass is accelerated. It usually only measures acceleration in one

direction but more than one may be grouped together for two or three dimensional measurements (Levine *et al.*, 2012).

Piezoelectric Accelerometers, represent the large class of dynamic vibration sensors that incorporate into one shielded package a Piezoelectric Transducer as a mechanical part and integral electronics as an electrical part (Barrett and Daniel, 2012; Anonymous, 2017a, b; Brozino and Donald, 2015; Levine *et al.*, 2012; Levinson, 2015; LTC, 2017; PCB Piezotronics, 2017; Bhattacharyya and Roy 2014; Stinson *et al.*, 2012; James, 2000; Xie, 2013) (Fig. 1).

Another known name for the same sensor is Integrated Circuit Piezoelectric (ICP) or Integral Electronics Piezoelectric (IEPE) Accelerometers. The advantages of an IEPE Accelerometer include low noise, wide dynamic range, wide frequency response, wide temperature range, low output impedance, high sensitivity and miniature design (Levinson, 2015)

A piezoelectric sensor generates an electric signal that is related on the dynamic change in the shape of the piezoelectric material as force is being applied. Thus, the piezoelectric materials can only directly measure time varying forces. A piezoelectric accelerometer is therefore,

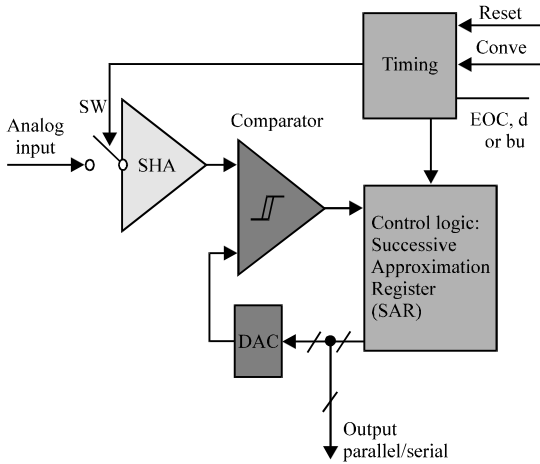


Fig. 1: Basic SAR ADC architecture (Xie, 2013)

better for measuring changes in acceleration instead of measuring constant accelerations (Brozino and Donald, 2014).

The other type of accelerometer is the Piezoresistive Accelerometer. Those are inertial sensors which measures acceleration of the reference frame to which they were attached (Bhattacharyya and Roy, 2014).

Piezoresistive shock accelerometers, manufactured by MEMS technology have low power consumption while still providing +/- 200 mV full scale output at acceleration levels >50 kg. The accelerometers are electrically compatible with the same type 4-wire circuit used to condition a strain gauge full bridge and since, they have much greater output compared to a strain gauge, the requirement for signal amplification is greatly reduced. It can afford a wider operating temperature range when compared to mechanically isolated ICP® accelerometers. Its frequency response were dependent on model that can be uniform from DC (0 Hz) to values as high as 20 kHz. To lessen the severity of response when their resonant frequency is excited they incorporate squeeze film damping, achieving values of 0.02-0.06 of critical. These damping values are much higher than those found in legacy MEMS accelerometers. Since, Silicon is a brittle material, over range stops are also, incorporated to minimize breakage of the sensing element and then the sensing element is sealed within a hermetic package. At comparable G levels, MEMS technology enables the smallest package size to be attained for individual accelerometers (PCB Piezotronics, 2017).

Piezoresistive Accelerometers design for high frequency, high G shock measurement. Instead of sensing the capacitance changes in the seismic mass a piezoresistive accelerometer takes advantage of the resistance change of piezoresistive materials to convert mechanical strain to a DC output voltage. Most of the piezoresistive designs were either MEMS type (gas

damped) or bonded strain gauge type (fluid damped) and they are suitable for impact measurements where frequency range and G level are considerably high.

Piezoresistive accelerometers were widely used in automobile safety testing including anti-lock braking system, safety air-bags and traction control system as well as weapon testing and seismic measurements. In addition, micromachined accelerometers were available and used in various applications such as submillimeter piezoresistive accelerometers in extremely small dimensions used for biomedical applications (Anonymous, 2017).

Since, that the piezoelectric and piezoresistive accelerometers produces reading of time-varying results, the use of a high resolution and high sampling rate A/D is being encouraged.

The successive approximation technique used a Digital to Analog Converter (D/A or D-A), a controller and a comparator to perform the A/D Conversion Process. Starting from the MSB down to the LSB, the controller turns in each bit at a time and generates an analog signal. Based on the result of the comparison, the controller changes or leaves the current bit and turns on the next MSB. The process continues until decisions are made for all the available bits (Barrett, and Daniel, 2012).

Successive approximation register A/D converters comprises of four main subcircuits: the Sample and Hold Amplifier (SHA), analog comparator, reference D/A converter and Successive Approximation Register (SAR). Because the SAR controls the converter operation, successive-approximation converters are often called SAR ADC's (Xie, 2013).

An important characteristic of SAR ADC is the end of the conversion time. The data corresponding to the sampling clock edge is available with no "pipeline" delay. The lack of "pipeline" delay (or latency) makes it ideal for single shot and multiplexed data acquisition applications.

Although, it is much slower than other models like the pipeline and flash ADC, power consumption is very low and a model of choice for low power devices (LTC., 2017).

MATERIALS AND METHODS

The proposed 32-bit resolution vibration, shock or impact data acquisition system will consist of the following: a 32-bit ARM Cortex M4F Microcontroller, +50/-50 G-force capacity Piezoelectric Shock Sensor as the main G-force measurement specimen, the latest 32-bit SAR A-D Converter and signal conditioning circuits for anti-aliasing and noise filtering.

Below is the complete schematic and block diagram of the proposed shock or impact 32-bit SAR data acquisition system.

Hardware design and software development: The block diagram at Fig. 2 and 3, the overview of the impact or Shock measurement system. The mainboard consists of the MSP432 ARM Cortex M4F microcontroller from Texas

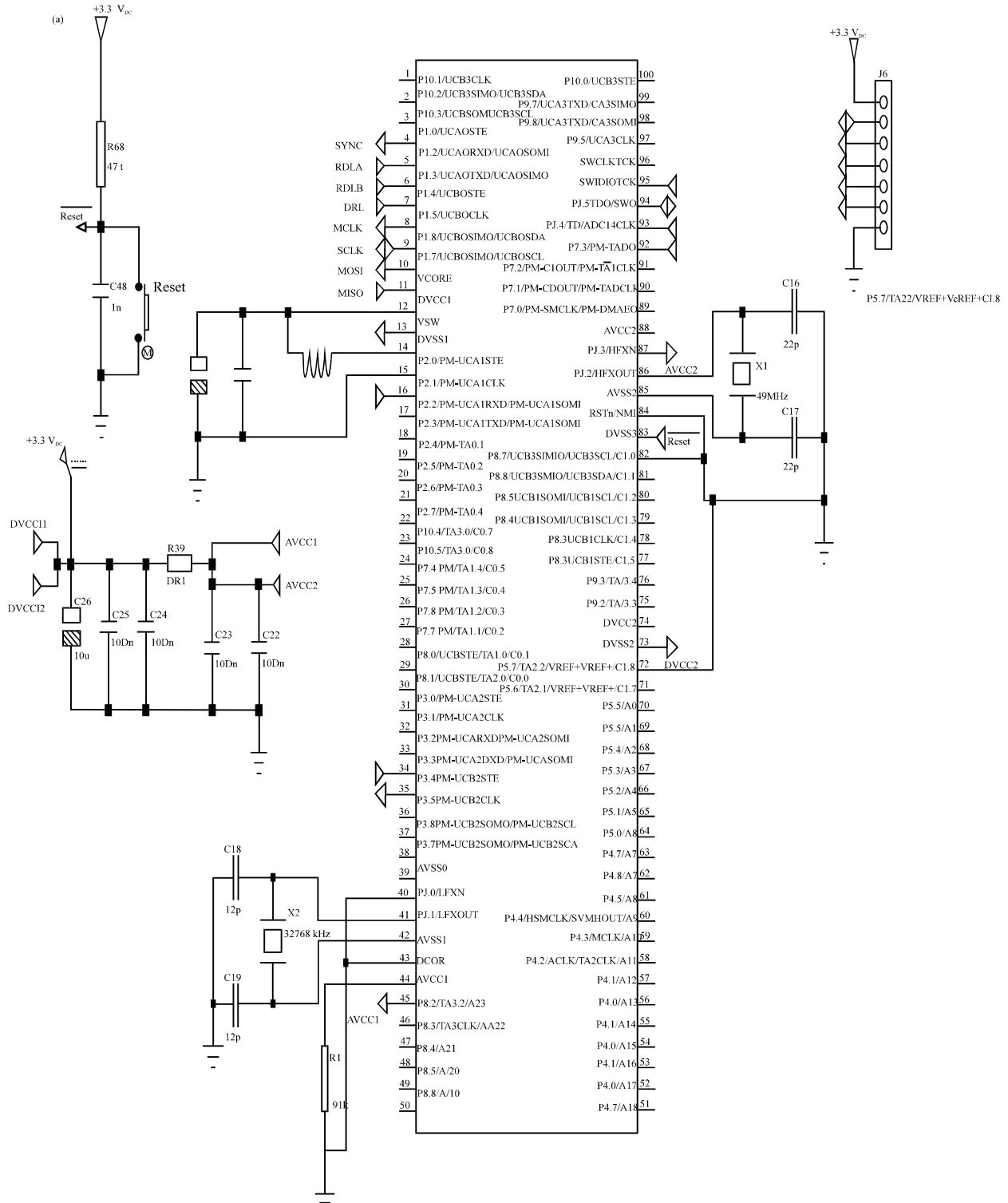


Fig. 2: Continue

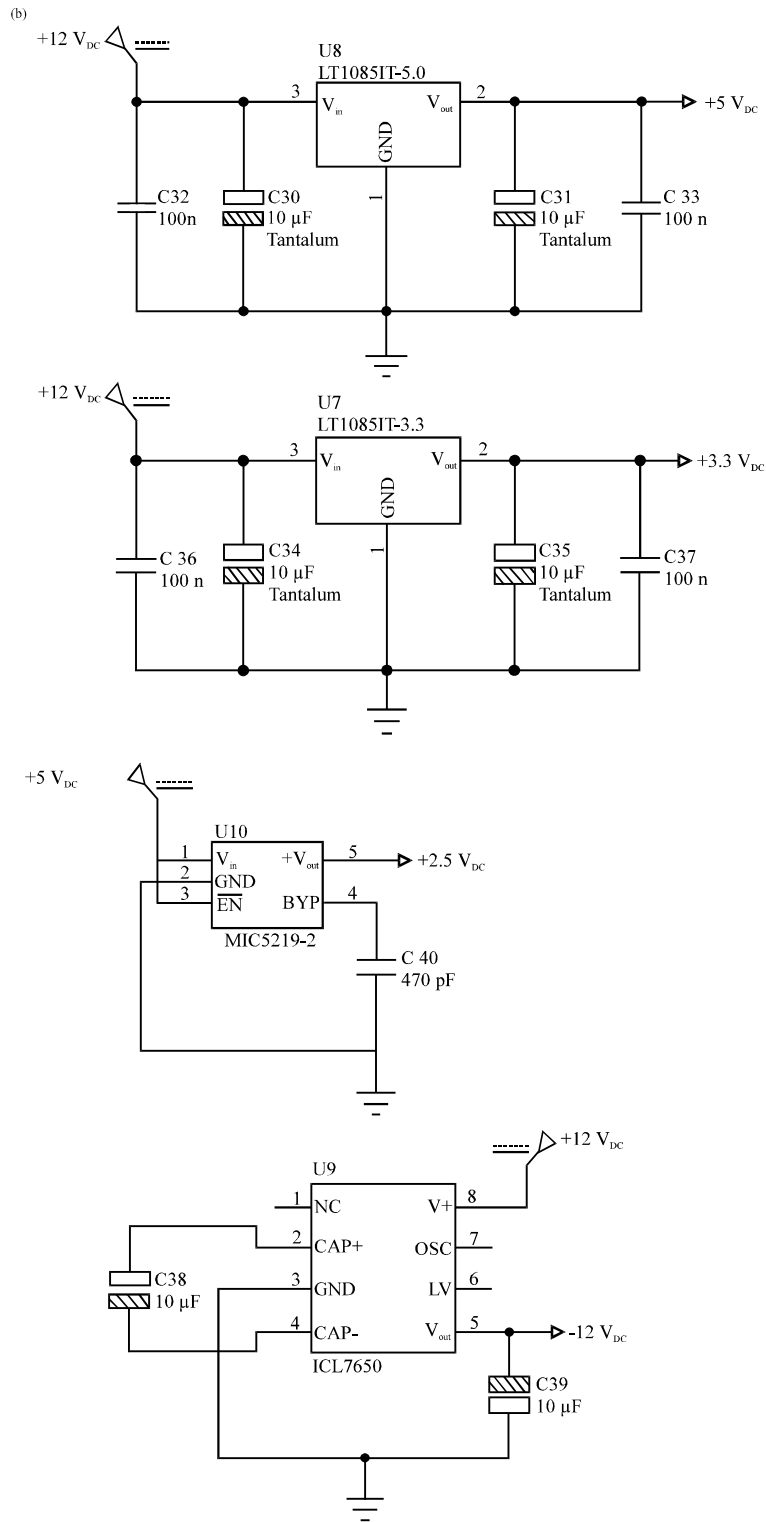


Fig. 2: Continue

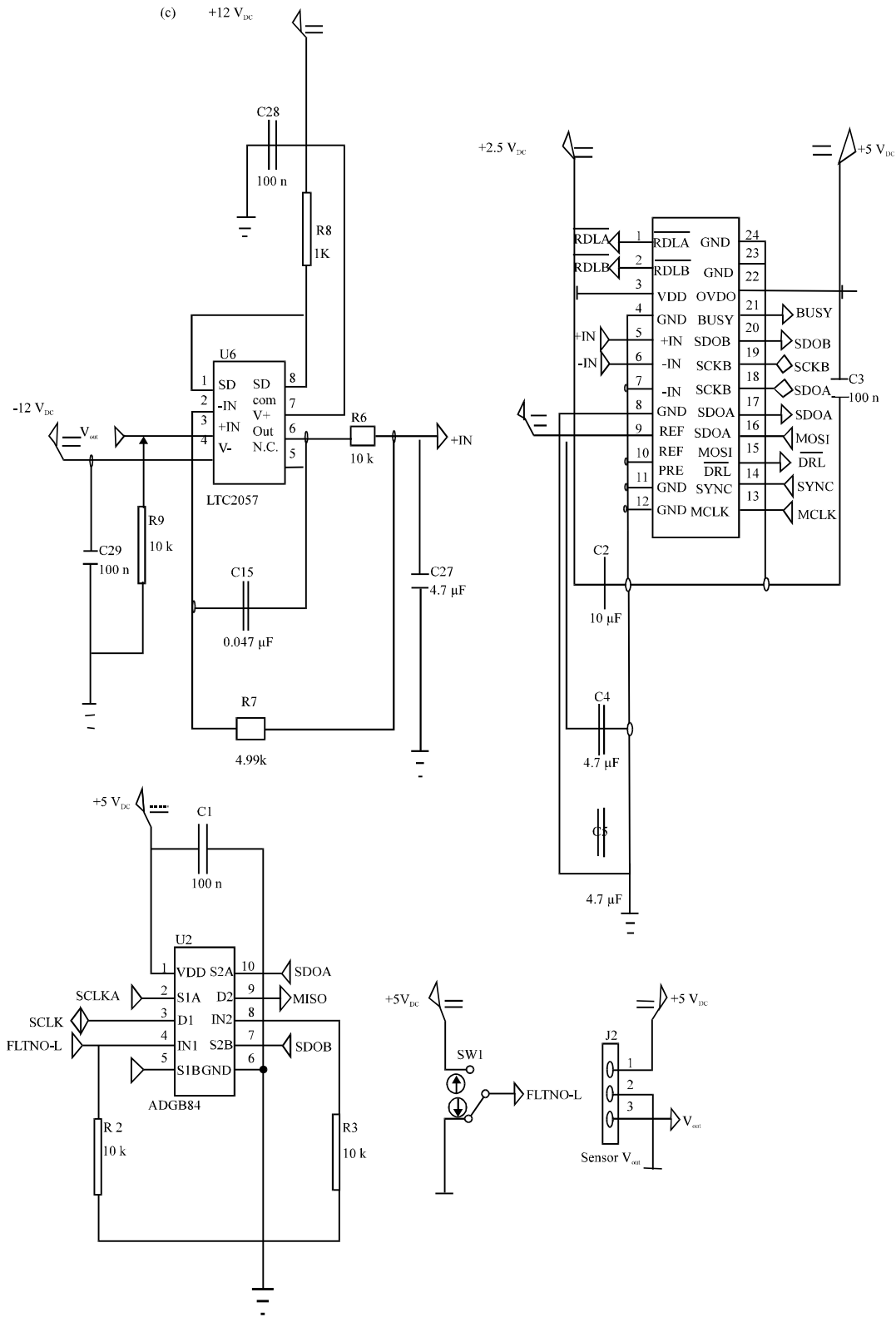


Fig. 2: Continue

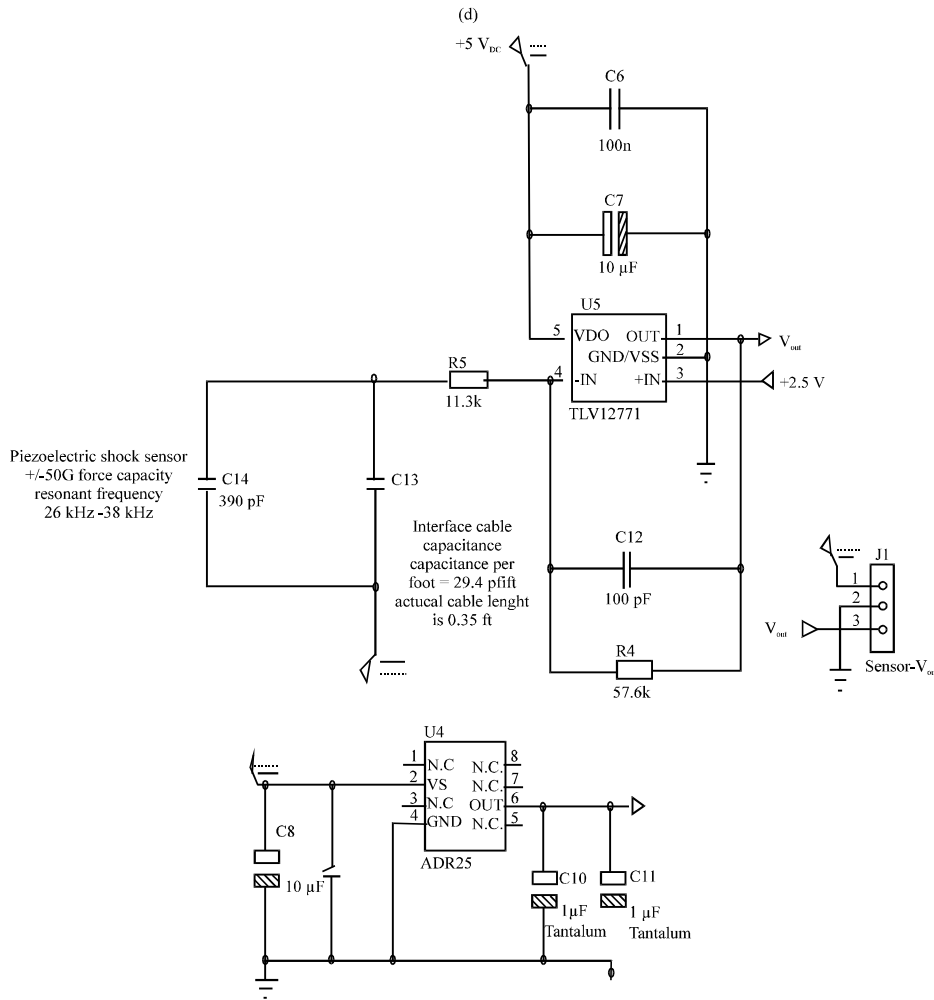


Fig. 2: a) MCU circuit; b) Power supply circuit; c) 32-bit SAR A/D circuit and d) Piezoelectric shock sensor node PCB circuit

Instruments© as the main processing unit. The UART port can be interfaced to a computer or to a HMI Display as desired.

The power supply section consists of Low Dropout Voltage regulators for producing voltages of +5 V_{DC}, +3.3 V_{DC} and +2.5 V_{DC} from a +12 V_{DC} input. The -12 V_{DC} will be produced by the ICL7660 from the +12 V_{DC} power supply to supply the LTC2057 Buffer Opamp.

The node PCB where the charge amplifier is currently located will be placed close to the Piezoelectric Shock Sensor PCB. The coaxial cable was intentionally shortened to minimize the effect of the cable capacitance which in turn significantly affects the high cutoff frequency of the charge amplifier. In this way, the output voltage of the charge amplifier can be easily buffered by an Opamp without being affected by the cable capacitance.

The software used to develop the firmware is Energia^{MT}. The commands are almost similar with Arduino© IDE. The difference is that Energia^{MT} can run multiple tasks at the same time.

Component calculations: The typical coaxial cable capacitance that is available on the market is 29.4 pF/ft. Since, that the Piezoelectric shock sensor is using 3inches away from the node PCB. This will contribute a 7.35 pF/ft of capacitance for the upper cutoff frequency of the charge amplifier:

$$\text{Capacitance} = 0.25 \text{ ft} \frac{29.4 \text{ pF}}{\text{ft}} = 7.35 \frac{\text{pF}}{\text{ft}} \quad (1)$$

For the lower cutoff frequency of the charge amplifier (Fig. 4). Assume following conditions:

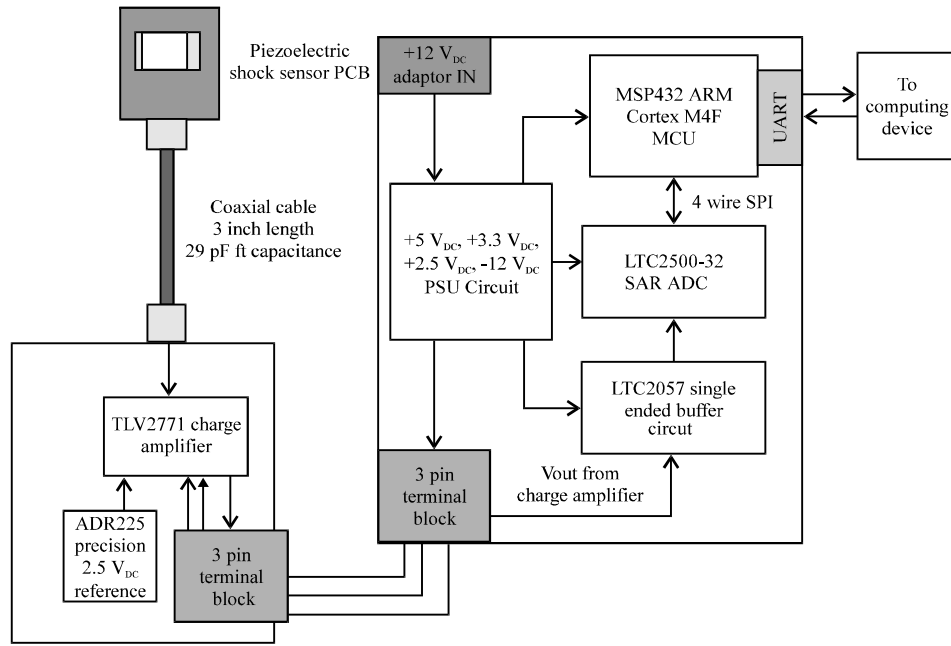


Fig. 3: Block diagram overview

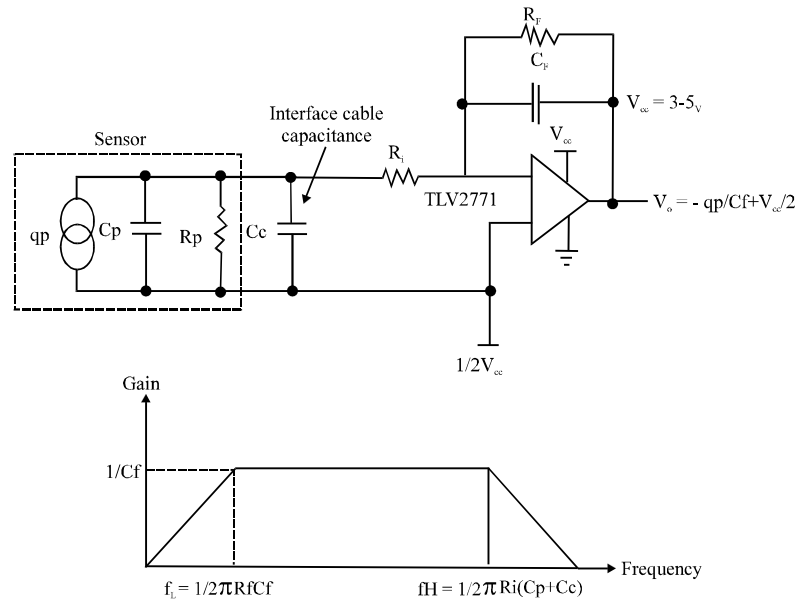


Fig. 4: Charge amplifier circuit

- 100 pF for “Cf”
- The lower resonant frequency of the piezoelectric shock sensor is 26 kHz
- Feedback resistor “Rf” is unknown

$$R_f = \frac{1}{2\pi f_L C_f} \quad (3)$$

$$f_L = \frac{1}{2\pi R_f C_f} \quad (2)$$

$$R_f = \frac{1}{2\pi (26000 \text{ Hz}) (100 \text{ pF})} \quad (4)$$

$$= 61213.43 \Omega$$

For the upper cutoff frequency of the charge amplifier. Assume following conditions:

- “Cp” is 390 pF and “Cc” is 7.35 pF
- Upper resonant frequency of the piezoelectric shock sensor is 36 kHz
- Input resistor “R_i” is unknown

$$f_H = \frac{1}{2\pi R_i (C_p + C_c)} \quad (5)$$

$$R_i = \frac{1}{2\pi f_H (C_p + C_c)} \quad (6)$$

$$R_i = \frac{1}{2\pi (36000 \text{ Hz})(390 \text{ pF} + 7.35 \text{ pF})} \quad (7)$$

$$= 11126.13 \Omega$$

The closest value can be selected are 11.3 kΩ for “R_i” and 57.6 kΩ for “R_f”.

The piezoelectric shock sensor produces a 0.35pC/G(qp) of charge with respect to the direction of “D” in the figure below. In this paper, +50G is feasible to measure on one axis location. The designer may group the sensors in different location.

Assuming that the charge amplifier has no input, the output voltage will be +2.5 V_{DC} if the supply Voltage (V_{cc}) is +5 V_{DC} and +1.8 V_{DC} when +3.6 V_{DC} is used.

When 1G of force is applied to the direction of “D” with respect to our calculation of components:

$$V_{out} = \frac{-qP V_{cc}}{Cf} \quad (8)$$

$$V_{out} = \frac{-0.35pC}{Cf} + \frac{+5.0V_{DC}}{2} \quad (9)$$

$$= 2.4965 V_{DC} \text{ at } 1G$$

The LTC 2500-32 transfer function of 32-bit A/D Converter is shown below (Fig. 5). The voltage for the LSB if +5 V_{DC} is applied on the V_{ref} pin is +2.3nV_{DC}. The output is in two’s complement format. This is calculated as:

$$LSB = \frac{2V_{ref}}{2^{32}} = \frac{2(+5.0V_{DC})}{4294967296} \quad (10)$$

$$= 2.3283064365386962890625e-9 V_{DC}$$

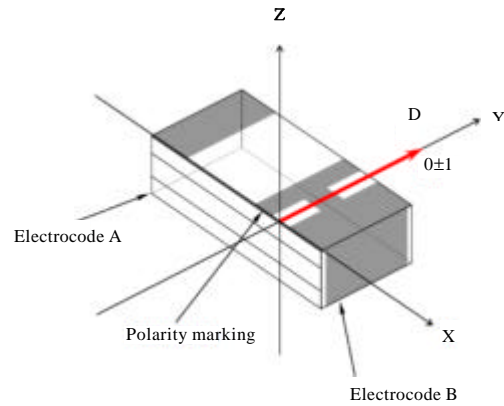


Fig. 5: Force applied on the “D” axis direction (Murata Manufacturing Co., Ltd.)

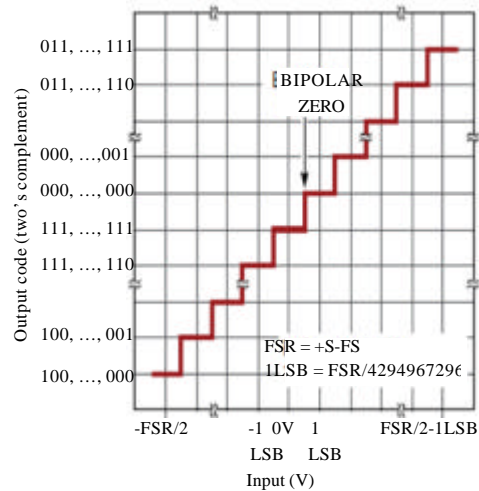


Fig. 6: LTC 2500-32 transfer function (Linear Technology Corporation, 2017)

RESULTS AND DISCUSSION

The LTC 2500-32 32-bit A/D converter has two operating modes that can be selected by the user. One is the filtered code output and the other is the no latency output. The difference between these two operating modes aside from the speed is the signal filters usage. The no latency code output cannot use the built-in digital filters. This A/D converter also can perform a traditional successive approximation register (sar) mode but 20 bits are guaranteed to be accurate (Fig. 6).

From the idle state of the charge amplifier, +2.5 V_{DC} is 0G or no input charge is present. The answer in Equation 9 produces a +2.4965 V_{DC} output at 1G of force applied in the direction of “D” axis. The voltage difference from 0-1 G is +0.0035 V_{DC}. The 32-bit A/D converter has an input

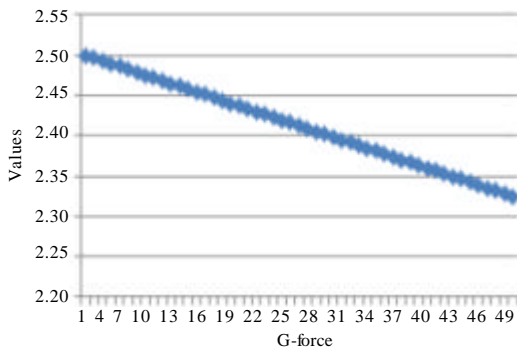


Fig. 7: Output voltage vs. G-force

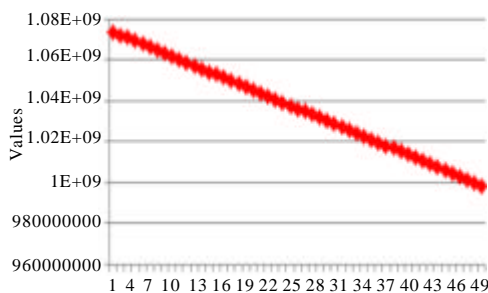


Fig. 8: ADC code vs. G-force

reference of $+5 V_{DC}$ and an LSB Voltage amounting to $+2.3 nV_{DC}$. The graph of charge amplifier output voltage with respect to the G-Force applied towards the “D” axis are below. As observed, the greater the force applied will lead to lower output voltage for the charge amplifier and ADC code output of the 32-bit A/D converter (Fig 6-8).

CONCLUSION

By using the latest ARM Cortex M4F 32-bit Microcontroller, the interfacing to different industrial protocols will be possible in one controller with multitasking capability.

There are two ways to read the Piezoelectric shock Sensor using a high slew rate opamp. One is the voltage amplifier mode and the other is the charge amplifier Mode. Charge amplifier mode was chosen to avoid the loss of accuracy due to the coaxial cables capacitance. By making the coaxial cable relatively short and buffering the output of the charge amplifier towards the input of the 32-bit A/D converter.

The 32-bit A/D Converter introduced in this study has a variety of features which can enhance the representation of the subject analog signal. This includes the relaxed anti-aliasing, FFT filter, decimation filters and modes of averaging and sampling that will make this system capable to adapt to any scenario sensitive measurement.

The output voltage of the charge amplifier and ADC code value are both inversely proportional to the charge generated of the Piezoelectric shock sensor reading a single axis of force applied towards the direction of “D” axis.

REFERENCES

- Anonymous, 2017a. Bestech sensors and teaching equipment. Bestech Australia, Dingley Village, Victoria. <http://www.bestech.com.au/piezoresistive/>.
- Anonymous, 2017b. Shock sensor PKGS-00GXP1-R, PKGS-00LDP1-R, PKGS-25SXAP1-R. Murata Manufacturing, Nagaokakyo, Kyoto Prefecture, Japan. <http://www.murata.com/en-us/products/sensor/guide/sensorguide3/sensorguide/pkggs>.
- Barrett, S.F. and J.P. Daniel, 2012. Atmel AVR Microcontroller Primer Programming and Interfacing. 2nd Edn., Morgan and Claypool Publishers San Rafael, California, USA., ISBN:9781608458615, Pages: 255.
- Bhattacharyya, T.K. and A.L. Roy, 2014. MEMS Piezoresistive Accelerometers. In: Micro and Smart Devices and Systems, Vinoy, K., G. Ananthasuresh, R. Pratap and S. Krupanidhi (Eds.). Springer, New Delhi, India, ISBN:978-81-322-1912-5, pp: 19-34.
- Bronzino, J.D. and R.P. Donald, 2014. Medical Devices and Human Engineering. 4th Edn., CRC Press, Boca Raton, Florida, USA., ISBN:9781138748569, Pages: 891.
- James, K., 2000. Signal conditioning piezoelectric sensor (Application report). Texas Instrument Incorporation, Texas, USA.
- LTC., 2017. LTC2500-32 32-bit over-sampling ADC with configurable digital filter. Linear Technology Corporation, Milpitas, California, USA.
- Levine, D., R. Jim and W. Michael, 2012. Whittle’s Gait Analysis. 5th Edn., Elsevier, Amsterdam, Netherlands, ISBN:9780702042652, Pages: 177.
- Levinzon, F., 2015. Piezoelectric Accelerometers with Integral Electronics. Springer, Berlin, Germany, ISBN:978-3-319-08077-2, Pages: 169.
- PCB Piezotronics, 2017. MTS systems corporation. PCB Piezotronics Inc., Depew, New York. <http://www.pcb.com/TestMeasurement/Accelerometers/mems>.
- Stinson, S., B. Barry and D.H. O’Rourke, 2012. Human Biology: An Evolutionary and Biocultural Perspective. 2nd Edn., Wiley-Blackwell, Hoboken, New Jersey, USA., ISBN-13:978-0470179642, Pages: 880.
- Xie, S., 2013. Successive-approximation ADCs: Ensuring a valid first conversion. Analog Devices, Norwood, Massachusetts, USA. <http://www.analog.com/en/analog-dialogue/articles/successive-approximation-adcs.html>.